THE JOURNAL OF BIOLOGICAL CHEMISTRY
Vol. 273, No. 16, Issue of April 17, pp. 9994–10003, 1998

Printed in U.S.A.

Insulin Receptor Substrate-1 is the Predominant Signaling Molecule Activated by Insulin-like Growth Factor-I, Insulin, and Interleukin-4 in Estrogen Receptor-positive Human Breast Cancer Cells*

(Received for publication, October 20, 1997, and in revised form, February 3, 1998)

James G. Jackson, Morris F. White‡, and Douglas Yee§

From the Division of Medical Oncology, Department of Medicine, University of Texas Health Science Center, San Antonio, Texas 78284-7884 and the ‡Research Division, Joslin Diabetes Center, Harvard Medical School, Boston, Massachusetts 02215

Because insulin-like growth factor-I (IGF-I), insulin, and interleukin-4 (IL-4) have known biological effects in breast cancer cells and signal through insulin-receptor substrate (IRS) adaptor proteins, we examined the expression and function of IRS-1 and IRS-2 in breast tumors and cell lines. IRS-1 and IRS-2 were expressed by cell lines and primary breast tumor specimens. IGF-I, insulin, and IL-4 treatment of MCF-7 and ZR-75, and IGF-I treatment of T47-D breast cancer cells, resulted in much greater tyrosine phosphorylation of IRS-1 compared with IRS-2. Furthermore, IGF-I stimulated greater tyrosine phosphorylation of IRS-1 than either insulin or IL-4. IGF-I treatment also enhanced association of the p85 regulatory subunit of phosphatidylinositol 3-kinase with IRS-1 and stimulated increased enzymatic activity compared with IL-4 and insulin in all three cell lines. Similarly, mitogen-activated protein kinase activity was greater in IGF-I-stimulated cells. To determine the functional significance of the activation of these pathways, we inhibited activation of phosphatidylinositol 3-kinase with wortmannin and mitogen-activated protein kinase with PD098059. Both compounds inhibited IGF-stimulated growth, suggesting that both pathways contributed to the mitogenic response to IGF-I. We conclude that IRS-1, and not IRS-2, is the predominant signaling molecule activated by IGF-I, insulin, and IL-4. Furthermore, enhanced tyrosine phosphorylation of IRS-1 by IGF-I, compared with either insulin or IL-4, is associated with greater activation of mitogenic downstream signaling pathways resulting in enhanced cell growth.

It has become clear that both insulin-like growth factor I (IGF-I)[1] and IGF-II stimulate both normal and malignant breast cell proliferation (1). Transgenic mice that overexpress IGF-II in mammary epithelial cells develop breast cancer, suggesting that IGF signaling may also participate in the transformation event (2). Most evidence suggests that the tyrosine kinase type I IGF receptor (IGFR1) mediates the mitogenic signaling of both IGF-I and IGF-II (3). Indeed, specific tyrosine residues contained in the intracellular domain of the receptor have been shown to mediate mitogenesis, transformation, and survival (4–6). Although insulin receptor also mediates a mitogenic signal for breast cancer cells (7), IGFR1 has been shown to stimulate a more potent mitogenic signal than the insulin receptor (8). Thus, identifying the key signaling pathways for IGFR1 may have implications for breast cancer.

Interest in characterizing the molecules that bind to the activated receptor has led to the discovery that multiple adaptor proteins are involved in IGF signal transduction. The adaptor protein insulin receptor substrate 1 (IRS-1) was one of the first molecules discovered (9); however, additional molecules (IRS-2, Shc, Crk, Gab10, GrbIR/Grb10, p85, and phosphatidylinositol 3-kinase (PI3 kinase)) have all been shown to interact directly with the receptor (10–13). Adding to this complexity, both IRS-1 and IRS-2 can couple to multiple additional signaling pathways (Grb2, p85, Syp, and Nck), which could potentially result in a cascade of signals originating from the IGFR1 (14). Recent results suggest that the IRS family may contain additional members (15, 16).

The IRS proteins were first identified as signaling molecules for the insulin receptor. Because IGFR1 is homologous to the insulin receptor, it was not surprising that both IRS-1 and IRS-2 are activated by the IGFs. However, additional ligands also activate the IRS proteins. Interleukin 4 (IL-4), a cytokine that stimulates B and T cell proliferation, also signals through the IRS proteins (17). Recent evidence has also shown that other cytokines also use the IRS-2 signaling pathway (18).

Because the pathways triggered by the IGFs and the signals mediated by the IRS adaptor proteins are complex, many of the studies demonstrating the function of these pathways have used transfection model systems. Although these systems are ideal for demonstrating protein-protein interactions, they are less well suited to identifying the biological effects of the activation of the signaling pathways. Interestingly, breast cancer cells have been shown to respond to IGF-I, IGF-II, and IL-4 (3, 19, 20). However, unlike lymphocytes, which respond to IL-4 by increased proliferation, breast cancer cells are inhibited by IL-4 treatment. Thus, breast cancer cells can be used to identify signaling pathways activated by both the IGFs and IL-4, and the activation of specific pathways can be coupled to the growth response of the ligand. This study had two aims: first, to determine which signaling molecules are activated by the mitogen IGF-I in breast cancer cells, and second, to determine how

* This work was supported by National Institutes of Health Grants P30 CA 54174 and PO1 CA 30195. The costs of publication of this article were defrayed in part by the payment of page charges. This article must therefore be hereby marked "*advertisement*" in accordance with 18 U.S.C. Section 1734 solely to indicate this fact.

§ Supported by Research Cancer Developmental Award KO4 CA 01670.
To whom correspondence should be addressed: Div. of Medical Oncology, Dept. of Medicine, University of Texas Health Science Center, 7703 Floyd Curl Dr., San Antonio, TX 78284-7884. Tel.: 210-567-4777; Fax: 210-567-6687; E-mail: doug@oncology.uthscsa.edu.

[1] The abbreviations used are: IGF, insulin-like growth factor; IGFR, IGF receptor; IRS, insulin receptor substrate; PI3 kinase, phosphatidylinositol 3-kinase; IL, interleukin; MAP, mitogen-activated protein; SFM, serum-free medium; TNESV, 50 mM Tris, pH 7.4, 1% Nonidet P-40, 2 mM EDTA, 100 mM NaCl, 10 mM sodium orthovanadate, 1 mM phenylmethylsulfonyl fluoride, 20 μg/ml leupeptin, 20 μg/ml aprotinin; PAGE, polyacrylamide gel electrophoresis; TBST, 0.15 M NaCl, 0.01 M Tris HCl, pH 7.4, 0.05% Tween 20; MTT, 3-(4,5-dimethylthiazol-2-yl)-2,5-diphenyl tetrazolium bromide.

IGF growth stimulatory and IL-4 growth inhibitory pathways differ in these cells.

Here we show expression of IRS-1 and IRS-2 in human breast cancer cells and primary breast tumors and that in estrogen receptor-positive cell lines, IRS-1 was the predominant signaling molecule activated by IGF-I, insulin, and IL-4. IGF-I, compared with either IL-4 or insulin, resulted in enhanced tyrosine phosphorylation of IRS-1. Furthermore, increased IRS-1 phosphorylation by IGF-I was directly correlated with increased activation of the downstream effector molecules PI3 kinase and mitogen-activated protein (MAP) kinase. Inhibition of PI3 kinase and MAP kinase activation showed that growth responses to IGF-I were mediated by both pathways. Thus, IRS-1 is the predominant signaling molecule phosphorylated by IGF-I, and multiple growth regulatory pathways are activated distally. Additionally, differences in the growth effects of IL-4 and IGF-I in breast cancer cells may be mediated by differential tyrosine phosphorylation of IRS-1.

EXPERIMENTAL PROCEDURES

Reagents—All chemicals and reagents were purchased from Sigma unless noted otherwise. IRS-1, IRS-2, MAP kinase, PI3 kinase, and 4G10 anti-phosphotyrosine antibodies were purchased from Upstate Biotechnology (Lake Placid, NY). Phospho-specific (activated) MAP kinase antibody was purchased from New England Biolabs (Beverly, MA), RC-20 anti-phosphotyrosine was purchased from Transduction Laboratories (Lexington, KY), and horseradish peroxidase-linked anti-rabbit antibody and rainbow molecular weight markers were from Amersham Pharmacia Biotech. Human interleukin 4 was from Collaborative Biomedical Products (Bedford, MA), IGF-I was from Gro Pep (Adelaide, South Australia, Australia), and insulin was from Novo Nordisk. Ortho[^{32}P]phosphate and [^{32}P]ATP were from NEN Life Science Products. Bisacrylamide was from Bio-Rad. PD 098059 was from Calbiochem. MCF-7, ZR-75, and T47-D cells were a gift of C. K. Osborne (San Antonio, TX). MDA-MB-231, MDA-MB-468, Hs578T, and Calu6 cells were purchased from ATCC (Rockville, MD). MDA-MB-435 cells were a gift from Nils Brünner (Finsenlab, Copenhagen, Denmark). Primary human breast cancers were obtained from the San Antonio Tumor Bank. These tissues were originally studied for steroid hormone receptor status, and excess tissue was stored as frozen, pulverized tumor powders at −70 °C.

Cell Stimulation and Lysis—Cells were cultured in improved minimal essential medium (Life Technologies, Inc.) with 10% fetal calf serum (Summit Biotech, Fort Collins, CO) and 10 nM insulin until 70% confluent and then washed twice with phosphate-buffered saline (Biofluids, Rockville, MD). For IRS-1 and IRS-2 blotting, cells were immediately lysed as described below. For stimulation experiments, medium was changed to serum-free medium (SFM) (described previously (21)) for 24–48 h. Cells were treated with PD098059 and wortmannin as described below, in growth assay. Medium was replaced with SFM plus indicated growth factors for 10 min at the following concentrations, unless noted otherwise: 5 nM IGF-I, 50 ng/ml IL-4, and 10 nM insulin. Cells were washed twice in ice-cold phosphate-buffered saline and lysed with 500 μl/10-cm dish TNESV buffer. Protein concentration of the cleared lysates was determined by the copper-bicinchoninic acid method with a kit from Pierce. Tumor proteins were also extracted in TNESV buffer as described previously (21).

Immunoprecipitations—All steps were performed on a platform rocker at 4 °C. Equal amounts of protein were first precleared with 25 μl of protein A-agarose for 30 min and then incubated with indicated antibody overnight at concentrations according to the manufacturer's instructions. 25 μl of protein A-agarose was then added for 4 h, followed by three washes with TNESV buffer. For anti-phosphotyrosine immunoprecipitations, 4G10-biotin was used followed by incubation with streptavidin-agarose beads. Beads were resuspended in 2× Laemmli loading buffer with 30 mg/ml dithiothreitol, boiled, and separated by SDS-PAGE (22).

Immunoblotting—After SDS-PAGE, proteins were transferred overnight to nitrocellulose membranes (Bio-Rad). The membranes were blocked in 5% nonfat dry milk in Tris-buffered saline-Tween 20 (TBST). For anti-phosphotyrosine blotting with RC-20, membranes were incubated with a 1000:1 dilution in buffer supplied for 2 h at room temperature and then washed five times with TBST. All other blots were incubated with a 1000:1 dilution of indicated antibody in blocking buffer for 1 h. Blots were then incubated with a 2000:1 dilution of horseradish peroxidase-linked anti-rabbit secondary antibody in blocking buffer for 1 h, followed by further washing. Enhanced chemiluminescence was performed according to the manufacturer's instructions (Pierce). Radiographic exposures for anti-phosphotyrosine and activated MAP kinase were typically 5–15 min, whereas MAP kinase, PI3 kinase, IRS-1, and IRS-2 were exposed for less than 1 min. Densitometry was performed by scanning the radiographs (ScanJet IIcx, Hewlett-Packard) and then analyzing the bands with ImageTool software, version 2.0 (University of Texas Health Science Center, San Antonio, TX).

V-8 Protease Digest—70% confluent cell monolayers were incubated overnight in SFM, washed twice with phosphate-free medium with no additives (Life Technologies, Inc.), and incubated for 1 h in the same medium. Medium was changed to phosphate-free medium with no additives plus 100 μCi/ml ortho[^{32}P]phosphate and incubated for 4 h; growth factor was added as indicated for 10 min, and then cells were lysed, immunoprecipitated, and separated by SDS-PAGE as described above. After electrophoresis, the gel was dried, and bands corresponding to IRS-1 were excised by aligning the gel with the autoradiogram. Gel slices were placed into wells and solubilized in buffer according to the method of Cleveland (23). 1.5 μg of V-8 protease was added to each well, and digestion occurred in the stacking gel. For anti-phosphotyrosine blotting of V-8 digests, IRS-1 immunoprecipitates were loaded directly into wells, digested as above, and transferred to nitrocellulose, and anti-phosphotyrosine blotting was performed as above.

PI3 Kinase Assay—After growth factor treatment, 70% confluent cell monolayers were washed, lysed, and incubated with primary antibody for 30 min followed by further incubation with protein A-agarose for 2 h according to the manufacturer's instructions (UBI). After last wash was removed, PI3 kinase assay was performed as described previously (24). Briefly, samples were resuspended in 50 μl of PI3 kinase buffer (20 mM Tris, pH 7.5, 100 mM NaCl, 0.5 mM EGTA), and 10 μg of phosphatidylinositol was added. After 10 min at room temperature, 10 μCi of [^{32}P]ATP and $MgCl_2$ to a final concentration of 20 μM were added. After 10 min at room temperature, lipids were extracted. The first extraction used 150 μl of $CHCl_3$:MeOH:HCl (10:20:0.2) followed by 100 μl of pure $CHCl_3$. The second extraction used 80 μl of MeOH:1N HCl (1:1). Samples were spotted on 1% potassium oxalate-treated TLC plates (Analtech, Newark, DE) and developed in $CHCl_3$:MeOH:NH_4OH:H_2O (129:114:15:21). Autoradiogram exposure was typically for less than 4 h. The highest migrating spots on the TLC plate, representing phosphatidylinositol phosphate, were quantitated on the AMBIS radioanalytic imaging system (San Diego, CA) or by PhosphorImager (Molecular Dynamics, Sunnyvale, CA).

Cell Proliferation Assay—Cells were grown in 24-well plates in full culture medium, changed to SFM overnight, and then changed to treatment groups and incubated as indicated in legends for Figs. 7 and 9. For wortmannin and PD098059 treatment, the compounds were diluted in Me_2SO and then added to SFM. The final concentration of the compound is indicated in Figs. 7 and 9; the final ratios were as follows: compound + Me_2SO, 0.33%; control groups, 0.33% Me_2SO alone. Growth factors were added after a 30-min preincubation with the inhibitor. Growth was analyzed using the 3-(4,5-dimethylthiazol-2-yl)-2,5-diphenyl tetrazolium bromide (MTT) assay (25). 60 μl of 5 mg/ml MTT reagent in phosphate-buffered saline was added to each well at the appropriate time point; then, after a 4 h incubation, wells were aspirated, and 0.5 ml of Me_2SO + 2.5% improved minimal essential medium was added. Absorbance was measured at 545 nm using a 690 nm differential filter.

RESULTS

IRS-1 and IRS-2 Were Expressed in Human Breast Cancer Cell Lines and Tumors—Because the IGFs can signal through multiple adaptor proteins, we first examined IRS-1 and IRS-2 expression in three estrogen receptor-positive (MCF-7, T47-D, and ZR-75) and four estrogen receptor-negative (MDA-231, MDA-468, MDA-435, and Hs578T) human breast cancer cell lines and one lung cancer cell line (Calu6). Six cell lines expressed high levels of IRS-1 (Fig. 1, *top panel*), and seven cell lines expressed IRS-2 (Fig. 1, *bottom panel*). Because we have previously shown IRS-1 expression in human breast tumors (21), we next examined human tumor specimens for IRS-2. Fig. 2, *top panel*, shows that all breast tumors examined expressed a 190-kDa protein detected by IRS-2 antiserum, similar in size to the single band seen in MCF-7 cell lysates. However, addi-

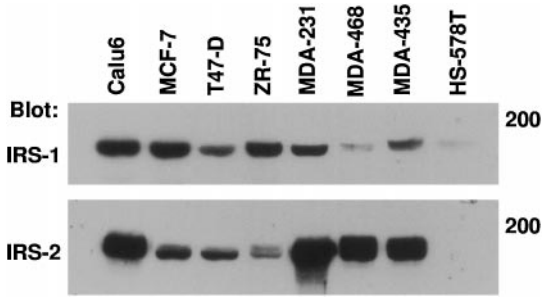

FIG. 1. **IRS-1 and IRS-2 expression by breast cancer cell lines.** Monolayers of breast cancer cell lines were lysed in TNESV buffer as described under "Experimental Procedures." 50 μg of total cellular protein was resolved by SDS-PAGE in duplicate and then blotted with IRS-1 (*top panel*) or IRS-2 (*bottom panel*) antibodies. Molecular weight markers are shown at the *right*.

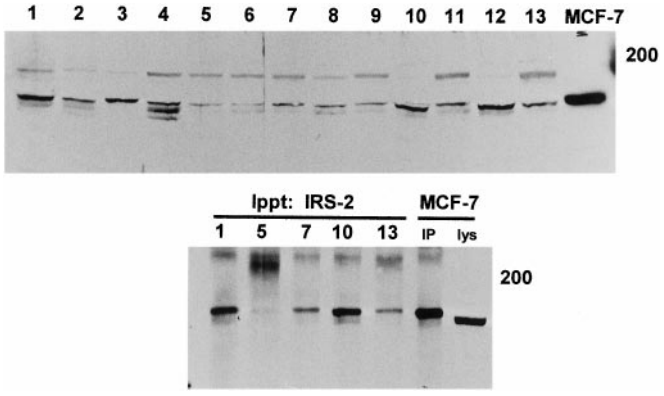

FIG. 2. **IRS-2 expression in breast tumors.** 50 μg of total protein from TNESV lysates of frozen pulverized breast tumors (*lanes 1–13*) and MCF-7 lysate (*MCF-7*) were analyzed by IRS-2 immunoblotting (*top panel*). Samples with varying levels of the 190-kDa protein detected by IRS-2 immunoblotting (500 μg of tumor (*lanes 1, 5, 7*, and *10*) or MCF-7 (*IP*) protein) were subjected to immunoprecipitation with IRS-2 antibody followed by immunoblotting (*bottom panel*) (MCF-7 total cell lysate (*lys*) was used as a control). Molecular weight markers are shown at the *right*.

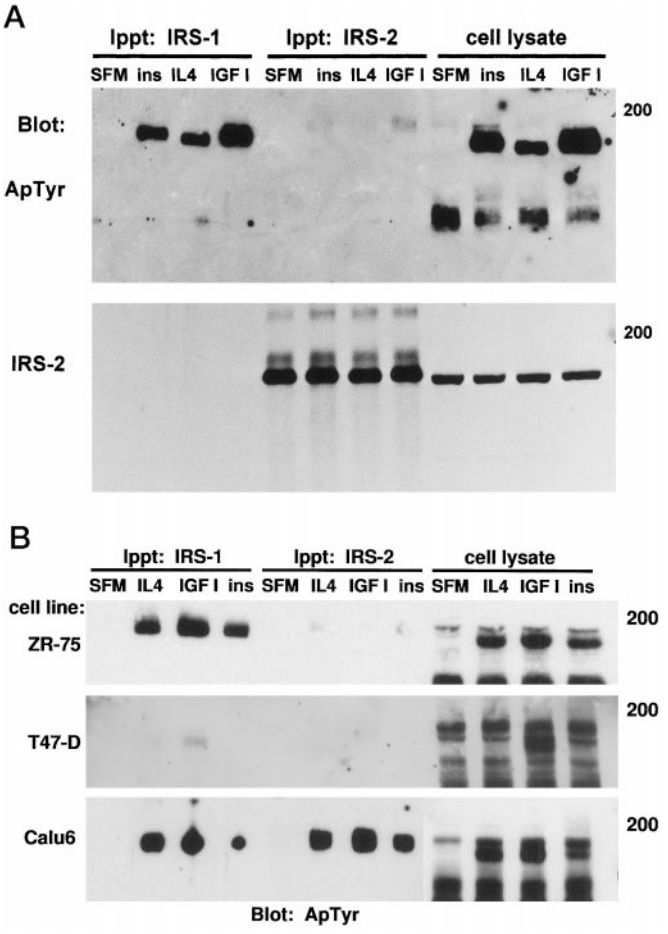

FIG. 3. *A*, IRS activation in MCF-7 cells. MCF-7 monolayers were untreated (*SFM*) or exposed to 10 nM insulin (*ins*), 50 ng/ml IL-4 (*IL4*), or 5 nM IGF-I (*IGF I*) for 10 min, and then lysates were immunoprecipitated with IRS-1 or IRS-2 antibodies and immunoblotted for anti-phosphotyrosine (*ApTyr, top panel*) followed by IRS-2 (*bottom panel*). In insulin-, IL-4-, and IGF-I-treated cells, anti-phosphotyrosine blotting shows a strong band at 185 kDa in the total cell lysates and in IRS-1 immunoprecipitated lanes but only a weak band at 190 kDa in IRS-2 immunoprecipitated lanes (*top panel*). IRS-2 blotting of the same membrane (*bottom panel*) shows that IRS-2 was present in IRS-2 immunoprecipitates and in cell lysates but not IRS-1 immunoprecipitates. *B*, IRS activation in ZR-75, T47-D, and Calu6 cells. Cell monolayers were analyzed exactly as in *A*. IRS-1 was strongly phosphorylated in IL-4-, IGF-I-, and insulin-stimulated ZR-75, whereas only a slight amount of IRS-2 phosphorylation was detected (*top panel*). In IGF-I-treated T47-D cells, phosphorylated IRS-1 but not IRS-2 was detected (*middle panel*). The lung cancer cell line Calu6 was included as a positive control for detection of phosphotyrosine on IRS-1 and IRS-2 after stimulation with each ligand (*bottom panel*).

tional bands were seen in some of the tumor samples. To confirm that the 190-kDa band in tumors was indeed IRS-2, we selected samples with varying levels of the 190-kDa protein and immunoprecipitated with IRS-2 antibody followed by immunoblot with the same antibody. Fig. 2, *bottom panel*, shows that following immunoprecipitation, a single band at 190 kDa was visualized for tumors and MCF-7 cells. The band in the immunoprecipitated lane correlated in intensity to the 190-kDa band in the total cell lysate of the same tumor specimen (Fig. 2, *top panel*).

We next determined the relationship between IRS-1 and IRS-2 expression by analyzing total cell lysates from breast tumor extracts. Nine of 10 breast tumors examined co-expressed IRS-1 and IRS-2 (data not shown). Given this co-expression of IRS-1 and IRS-2 in breast cancer cell lines as well as tumors, our next objective was to determine which substrate, if any, predominates in IGF-I, insulin, and IL-4 signaling in breast cancer cells.

IRS-1, IRS-2, and Shc Activation in Breast Cancer Cells—Initially, we used the IGF-I-, IL-4-, and insulin-responsive, estrogen receptor-positive breast cancer cell line MCF-7 to examine postreceptor signaling. As shown, this cell line expresses IRS-1 and IRS-2, as determined by immunoblotting (Fig. 1). Anti-phosphotyrosine blotting (Fig. 3*A, top panel*) detected a prominent 185–190-kDa phosphorylated protein in total cell lysates of insulin-, IL-4-, and IGF-I-treated cells, but not in untreated cells (SFM). To determine the identity of this phosphoprotein, we immunoprecipitated cell lysates with IRS-1 and IRS-2 antibodies, followed by anti-phosphotyrosine immunoblotting. IRS-1 antibody immunoprecipitated a 185-kDa phosphotyrosine-containing protein in cells treated with insulin, IL-4, and IGF-I but not in untreated cells (Fig. 3*A, top panel*). IRS-2 antibody immunoprecipitated a faint, 190-kDa phosphotyrosine reactive band in the IGF-I- and insulin-treated cells. Although IRS-2 protein was present in the IRS-2 immunoprecipitates and in the total cell lysates (Fig. 3*A, bottom panel*), little tyrosine phosphorylation was seen after exposure to any of the ligands. No IRS-2 was detected in IRS-1 immunoprecipitates. Furthermore, as seen in Fig. 3, IGF-I caused IRS-1 to migrate at a slower rate compared with IL-4-stimulated IRS-1, suggesting that IGF-I caused a higher degree of tyrosine phosphorylation.

As Fig. 1 shows, IRS-1 and IRS-2 were also co-expressed in

several other breast cancer cell lines. After demonstrating IRS-1 activation in MCF-7 cells, we next investigated two more IGF-I-responsive, estrogen receptor-positive cell lines, ZR-75 and T47-D (26, 27). Fig. 3*B, top panel*, shows that IL-4, IGF-I, and insulin stimulated a prominent 185–190-kDa phosphoprotein in the total cell lysates of ZR-75. After IRS-1 immunoprecipitation, a 185–190-kDa phosphoprotein was present in IL-4-, IGF-I-, and insulin-treated lanes but not in untreated cells (SFM). After stimulation by all three ligands and IRS-2 immunoprecipitation, only a faint tyrosine-phosphorylated band was identified. T47-D, another estrogen receptor-positive cell line, showed IRS-1 and no IRS-2 phosphorylation after IGF-I treatment. Of note is that tyrosine phosphorylation of IRS-1 or IRS-2 was not detected in response to IL-4 and insulin (Fig. 3*B*). However, the pattern of IRS-1 activation instead of IRS-2 after IGF-I treatment in T47-D cells was very similar to that of ZR-75 and MCF-7.

To show that IRS-2 antibody could immunoprecipitate phosphorylated IRS-2, we stimulated the lung cancer cell line Calu6 with the three ligands and blotted for anti-phosphotyrosine. A 185–190-kDa phosphorylated protein was seen in the whole cell lysates of IL-4-, IGF-I-, and insulin-treated cells (Fig. 3*B, lower panel*). Immunoprecipitation with IRS-1 antibody revealed a single band phosphoprotein at 185 kDa in the treated lanes, similar to MCF-7 cells. In contrast to the breast cancer cell lines, IRS-2 antibody also immunoprecipitated a 190-kDa phosphoprotein in Calu6. In these treated cells, IRS-1 and IRS-2 antibodies immunoprecipitated bands of similar relative intensity after blotting with anti-phosphotyrosine antibodies. Under the same conditions in MCF-7, ZR-75, and T47-D cells, IRS-1 antibodies immunoprecipitated a strong tyrosine-phosphorylated band, whereas IRS-2 antibodies immunoprecipitated only a weak band or none at all. Using the same antibodies in immunoblotting (Fig. 1), it is clear that IRS-1 and IRS-2 are expressed in these cells (Calu6, MCF-7, T47-D, and ZR75).

Although there were apparent differences in relative levels of the IRS-1 and IRS-2 among the cell lines, immunoblotting with two different antibodies cannot be used to make quantitative statements about the relative abundance of IRS-1 *versus* IRS-2 within a single cell line. However, it was our impression that the levels of phosphorylation of IRS-1 compared with IRS-2 in the IGF-responsive cell lines were greater than their absolute level of expression would suggest. To further evaluate this possibility, we measured total and phosphorylated levels of IRS-1 and IRS-2 by densitometry. If levels of phosphorylation were directly related to the absolute levels of protein, we would expect that the ratio of phosphorylated IRS-2 to phosphorylated IRS-1 would be similar to the ratio of total IRS-2 to total IRS-1. To estimate these values, we used Calu6 cell lysates as a standard and arbitrarily set the level of IRS expression in Calu6 cells to a value of 1. We determined that in phosphotyrosine blotting of Calu6, IRS-2/IRS-1 was 0.78, close to the arbitrarily defined ratio of total levels of IRS-2:IRS-1 of 1. IRS-1 levels in MCF-7 were 92% of Calu6 levels, and IRS-2 levels were 40%; therefore, based on the Calu6 model, their predicted ratio of activation when adjusted for the total IRS levels would be $0.4/0.92 \times 0.78 = 34\%$. However, the actual ratio of phosphorylated IRS-2:IRS-1 was only 2%. In other words, MCF-7 expresses nearly equal IRS-1 and just under half the IRS-2 of Calu6, yet instead of having 3 times as much IRS-1 activated, it had 50 times as much IRS-1 activated as IRS-2. Similar results were found for ZR-75, but T-47D did not activate IRS-2 at all, so no ratio could be calculated. Of course, even though one would predict IRS-2 activation would be higher in MCF-7 and ZR-75, one cannot completely rule out that the reduced levels of IRS-2 were still responsible for the weak level of activation. Differences in how phosphotyrosine antibodies react with phosphorylated IRS-1 and IRS-2 and how IRS-1 or IRS-2 antibodies react might also explain the differences in IRS-2 activation observed in MCF-7 and Calu6. Nonetheless, we conclude that IRS-1 is the predominant signaling molecule activated by IGF-I in these breast cancer cells.

In the estrogen receptor-negative cell lines MDA-231, MDA-468, MDA-435, and Hs-578T, IRS-1 activation was only minimally detected or not detected at all after ligand treatment, similar to the situation for IRS-2 in the estrogen receptor-positive cell lines (data not shown). These estrogen receptor-negative cell lines are not growth stimulated by IGF-I, whereas the estrogen receptor-positive cell lines MCF-7, ZR-75, and T47-D (28, 29) are all reported to be responsive to IGF-I and all appear to predominantly use IRS-1 activation as a signaling mechanism. It has been previously shown that MDA-231 and MDA-468 cells have postreceptor defects in the insulin and IGF signaling pathway (30, 31).

Shc has been previously reported to bind directly to IGFR1 (10, 32) and insulin receptor to stimulate mitogenesis independently of IRS-1 in L-6 myoblasts (33) and in 32D cells (34). Although Shc was detectable by immunoblot in MCF-7 cells, immunoprecipitation followed by anti-phosphotyrosine blotting did not detect Shc activation after IGF-I treatment (data not shown). In contrast, epidermal growth factor treatment of the MDA-MB-231 breast cancer cell line stimulated Shc phosphorylation (data not shown). Therefore, Shc signaling may be important in mediating the biological effects of different growth factors, but it does not appear to be activated by IGF-I in the IGF-responsive MCF-7 cells.

Thus, our data show that IRS-1 is the predominant tyrosine-phosphorylated protein species in the estrogen receptor-positive cell lines T47-D (stimulated with IGF-I), MCF-7, and ZR-75 (stimulated with insulin, IL-4, and IGF-I). Because these ligands have diverse biological effects, we next examined how each effected tyrosine phosphorylation of IRS-1 in MCF-7 cells.

IGF-I, Insulin, and IL-4 Stimulated Different Patterns of Phosphorylation of IRS-1—Regulation of downstream signaling elements through differential tyrosine phosphorylation of IRS-1 by insulin and IL-4 has been suggested previously (35). Because the migration pattern of IRS-1 was different when stimulated by each ligand, we next asked whether this difference could be due to phosphorylation, and specifically, to phosphorylation on tyrosine residues. To determine this, we immunoprecipitated IRS-1 from stimulated, ^{32}P-labeled cell lysates of MCF-7 cells. 185-kDa bands corresponding to IRS-1 (Fig. 4, *left panel*) were excised and digested with V-8 protease (Fig. 4, *middle panel*). After V-8 digestion, a fragment of 43 kDa appeared to increase in intensity from unstimulated (SFM), to IL-4 and insulin, to IGF-I. The unstimulated cells (SFM) before and after digestion had a high level of basal phosphorylation of IRS-1 (Fig. 4, *left* and *middle panels*), but tyrosine phosphorylation of IRS-1 was not detected by anti-phosphotyrosine blotting in these lysates of unstimulated cells. In contrast, treated cells consistently showed a prominent tyrosine-phosphorylated band at 185 kDa (data not shown). These findings suggest that IRS-1 has a high degree of basal serine/threonine phosphorylation and that the increased intensity of the 43-kDa V-8 fragment is likely due to enhanced tyrosine phosphorylation. To test this, we directly digested IRS-1 immunoprecipitates with V-8 protease and analyzed the fragments by antiphosphotyrosine immunoblotting. Fig. 4 (*right panel*) shows a 43-kDa band present in treated cells but not in the untreated samples. This band appeared to co-migrate with the 43-kDa doublet seen in ^{32}P-labeled IRS-1 V-8 fragments (Fig. 4, *middle panel*). The intensity of this fragment was greater in IGF-I-treated cells

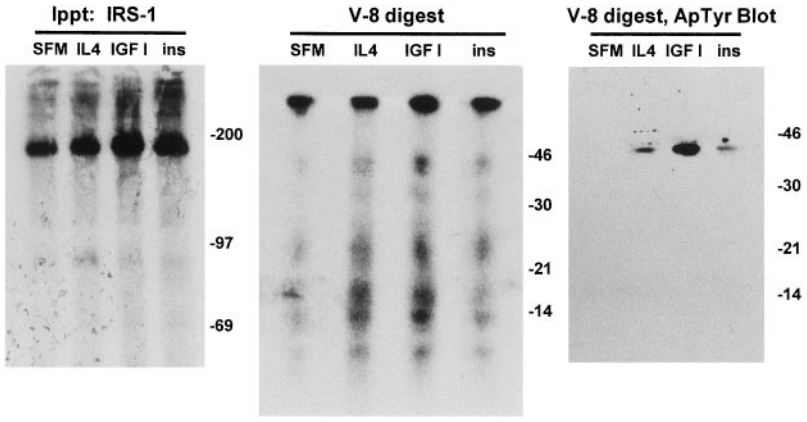

FIG. 4. **V-8 digest of IRS-1.** MCF-7 monolayers were labeled with ortho[^{32}P] phosphate as described under "Experimental Procedures"; then, IRS-1 immunoprecipitates were separated by SDS-PAGE, and the gel was dried and exposed to x-ray film (*left panel*). Bands corresponding to [^{32}P]IRS-1 (at approximately 185 kDa) were excised from the dried gel, digested with V-8 protease, and resolved by SDS-PAGE (*middle panel*). In the right panel, IRS-1 immunoprecipitates of lysates from treated cells were directly V-8 digested, resolved by SDS-PAGE, and then anti-phosphotyrosine immunoblotted. Molecular weight markers are shown at the *right* of each gel.

than in either IL-4-treated or insulin-treated cells, suggesting that this fragment was more heavily tyrosine-phosphorylated by IGFR1. We next examined whether this observed increase in tyrosine phosphorylation of IRS-1 resulted in increased activation of two well-characterized effectors of IGF action, PI3 kinase and MAP kinase.

IGF-I, Insulin, and IL-4 Increased the Association between IRS-1 and PI3 Kinase— To determine whether signaling events distal to IRS-1 are differentially activated by IGF-I, insulin, and IL-4, we first examined the effects of each ligand on the p85 regulatory subunit of PI3 kinase. In Fig. 5*A*, antibodies against the p85 regulatory subunit of PI3 kinase and IRS-1 both immunoprecipitated a 185-kDa phosphotyrosine band consistent with IRS-1 in MCF-7 cells. In Fig. 5*B*, IRS-1 immunoprecipitates and whole cell lysates were blotted with PI3 kinase antibodies. In MCF-7, ZR-75, and T47-D cells, treatment with IGF-I greatly increased the association of PI3 kinase with IRS-1 (Fig. 5*B, left panels*). IL-4 and insulin increased this association compared with untreated cells (SFM) but did not increase it to levels equal to IGF-I. PI3 kinase levels were equal in the total cell lysates of each treatment group (Fig. 5*B, right panels*). In T47-D cells, the ratio of PI3 kinase that co-immunoprecipitated with IRS-1 to the amount present in total cell lysates detected by immunoblotting (Fig. 5*B, bottom panels*) was comparatively smaller than the ratios in MCF-7 or ZR-75. This is consistent with the finding, shown in Fig. 3*B*, that IGF-I-stimulated tyrosine phosphorylation of IRS-1 was not as easily detected in T47-D cells as in MCF-7 or ZR-75 cells.

IGF-I, Insulin, and IL-4 Activation of PI3 Kinase—To verify that the observed increased IRS-1/PI3 kinase association also increased biochemical activation of PI3 kinase, a PI3 kinase assay was performed. Fig. 6*A* shows that IGF-I stimulated a marked increase in PI3 kinase activity over untreated cells (SFM), whereas IL-4 and insulin were less effective activators. Increased PI3 kinase activity was detected both in IRS-1 (Fig. 6*A, right panel*) and anti-phosphotyrosine (*left panel*) immunoprecipitates. Fig. 6*B* shows that PI3 kinase activity in ZR-75 and T47-D cells was also markedly increased with IGF-I treatment, whereas IL-4 and insulin were less effective. In T47-D cells, the activation of PI3 kinase was minimal after treatment with either IL-4 or insulin, which is consistent with the finding that IRS-1 is phosphorylated minimally or not at all after treatment with these ligands (Fig. 3*B*). These data suggest that the increased tyrosine phosphorylation of IRS-1 seen in phosphotyrosine blotting (Fig. 3) and V-8 digests (Fig. 4) correlates with increased PI3 kinase association with IRS-1 (Fig. 5) and PI3 kinase enzymatic activity (Fig. 6).

Inhibition of PI3 Kinase Signaling in Estrogen Receptor-positive Cell Lines—To examine the contribution of PI3 kinase to the IGF-I-mediated proliferative signal, we employed the

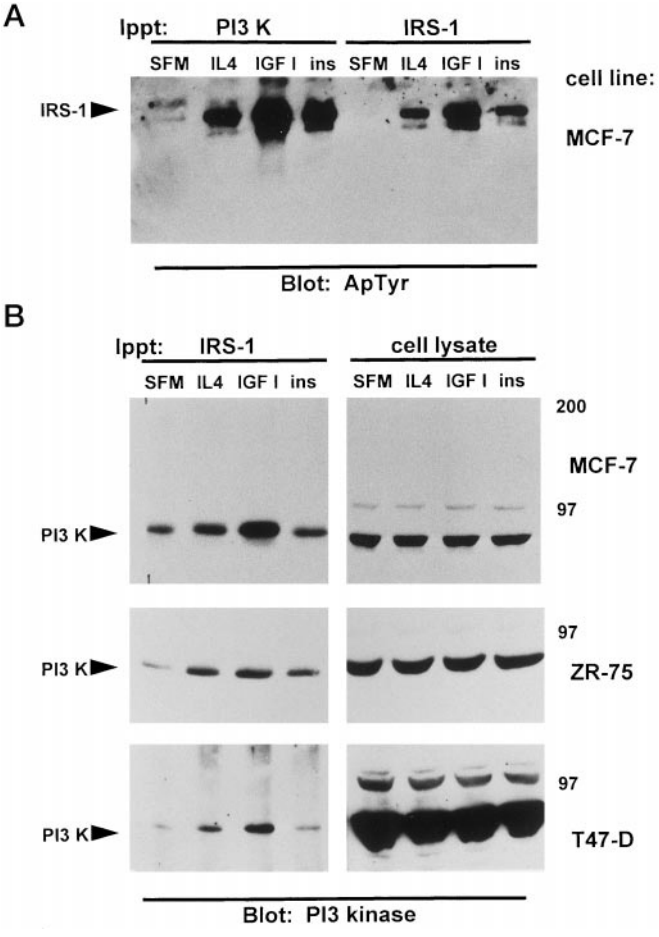

FIG. 5. **IRS-1 association with PI3 kinase.** *A*, MCF-7 monolayers were treated as indicated *above* lanes, and TNESV lysates were immunoprecipitated with PI3 kinase or IRS-1 antibodies, followed by anti-phosphotyrosine immunoblotting. Phosphorylated IRS-1 (indicated at the *left*) was detected in both the PI3 kinase and IRS-1 immunoprecipitates. *B*, MCF-7, ZR-75, and T47-D monolayers were treated as indicated *above* lanes, and TNESV lysates were immunoprecipitated with IRS-1 antibodies, followed by p85 PI3 kinase immunoblotting. 50 μg of total protein from cell lysates was included to show equal levels of PI3 kinase before IRS-1 immunoprecipitation in each treatment group (*cell lysate*).

specific inhibitor wortmannin to block PI3 kinase activation (36). Wortmannin caused a dose-dependent decrease in basal and IGF-I-stimulated PI3 kinase activity in MCF-7 cells (Fig. 7*A*). Dose-dependent inhibition of basal and IGF-I-stimulated growth by wortmannin (Fig. 7*B*) mirrored the biochemical inhibition (Fig. 7*A*). Complete inhibition of IGF-I-induced PI3

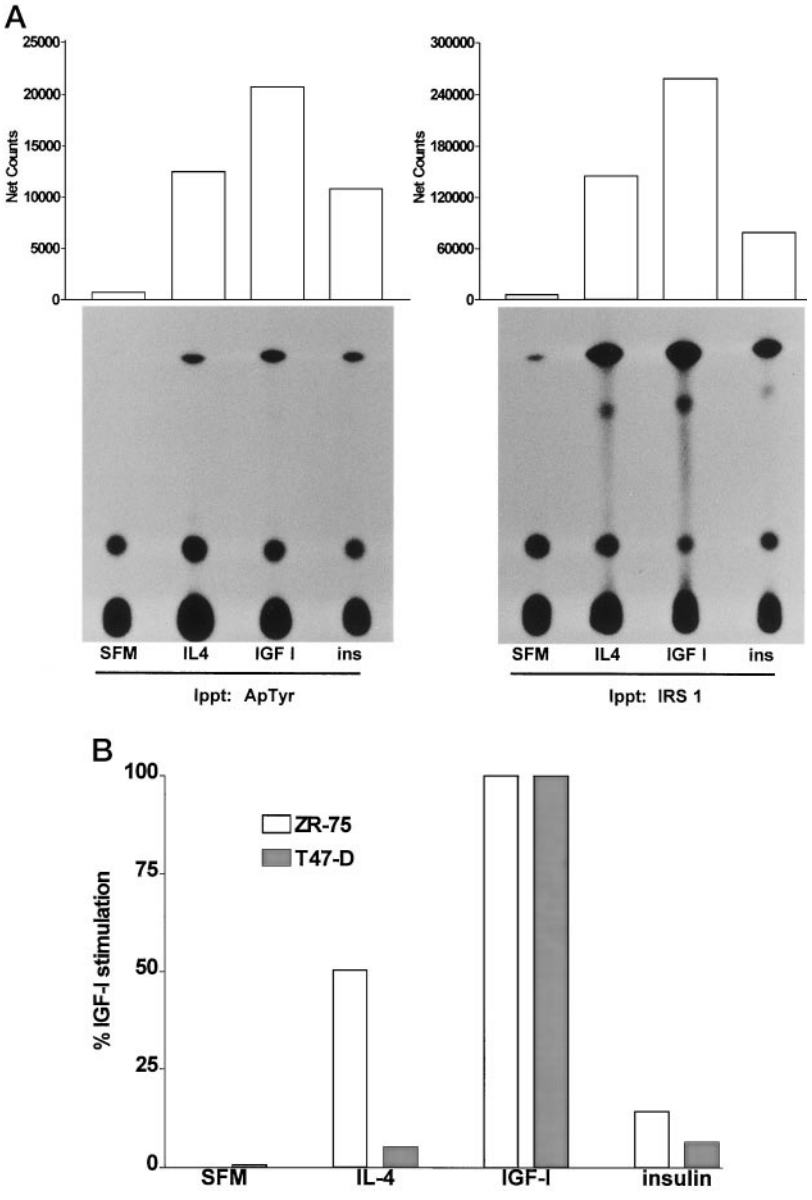

FIG. 6. *A*, PI3 kinase activation in MCF-7 cells. MCF-7 monolayers were treated as indicated *below* lanes and then lysed, immunoprecipitated with either anti-phosphotyrosine (ApTyr) or IRS-1 antibodies, and assayed for PI3 kinase activity as described under "Experimental Procedures." Individual spots representing phosphatidylinositol phosphate (the highest spot on the TLC plate) were quantitated on an AMBIS radioanalytic system, and the net counts for each spot are represented on the *graphs*. *B*, PI3 kinase activation in ZR-75 and T47-D cells. Cells were treated as indicated and immunoprecipitated with IRS-I antibody, and PI3 kinase assay was performed as in *A*. Labeled phosphatidylinositol phosphate was quantitated using a PhosphorImager (*ZR-75*) or AMBIS (*T47-D*) and are expressed as a percentage of IGF-I stimulation.

kinase activity or growth could not be achieved at any concentration of wortmannin. 250 nM wortmannin also decreased IL-4- and insulin-stimulated PI3 kinase activity in MCF-7 cells in a manner similar to that shown for IGF-I (data not shown). Fig. 7*C* shows that IGF-I-induced PI3 kinase activity in ZR-75 and T47-D could also be blocked by 250 nM wortmannin. IGF-I-stimulated growth in ZR-75 cells (approximately 1.7 times control; average of three experiments) was also partially blocked by 250 nM wortmannin (data not shown). Thus, IGF-I activation of PI3 kinase was associated with mitogenesis. We next examined the activation of another downstream signaling pathway important in mitogenic stimulation, MAP kinase.

IGF-I-, Insulin-, and IL-4-stimulated Activation of MAP Kinase—Phosphorylated IRS-1 can activate the MAP kinase pathway by binding Grb2 and engaging the ras/raf pathway (37). In MCF-7 cells, stimulation by IGF-I and the phorbol ester 12-*O*-tetradecanoylphorbol-13-acetate (*TPA*) resulted in phosphorylation of the p44 and p42 (erk1 and erk2) members of the MAP kinase pathway, whereas IL-4, insulin, and 10% serum were less effective (Fig. 8, *top panel*). Total MAP kinase blotting showed that levels of MAP kinase were equal in all of the cell lysates (Fig. 8, *bottom panel*). Thus, MAP kinase, like PI3 kinase, was more vigorously activated by IGF-I than by insulin and IL-4. Because IGF-I stimulated activation of MAP kinase, we next tested whether this pathway contributed to the proliferative signal delivered by IGF-I.

To block activation of the MAP kinase pathway, we used the MAP kinase activating enzyme inhibitor PD098059 (38). MAP kinase activating enzyme inhibition by PD098059 had no effect on activation of IRS-1 (Fig. 9*A, top panel*) but decreased IGF-I, IL-4, insulin, and 12-*O*-tetradecanoylphorbol-13-acetate stimulation of MAP kinase in MCF-7 cells (Fig. 9*A, bottom panel*). The inhibition of MAP kinase activation by PD098059 resulted in a dose-dependent reduction of IGF-I-stimulated growth in MCF-7 cells (Fig. 9*B*). Very similar results were found in ZR-75 and T47-D (Fig. 9*C*). IGF-I treatment resulted in an increased activation of MAP kinase compared with IL-4 or insulin treatment, and activation of MAP kinase by all three ligands was partially blocked by preincubation with PD098059. IGF-I-induced growth of ZR-75 cells was similarly partially blocked by PD098059 preincubation (data not shown). Thus, MAP kinase and PI3 kinase are stimulated by IGF-I in these breast cancer cell lines and contribute to the mitogenic response.

Excess Insulin but Not Excess IL-4 Increased IRS-1, MAP Kinase, and PI3 Kinase Activation—To determine whether IL-4 or insulin could mimic IGF-I actions at excess concentrations,

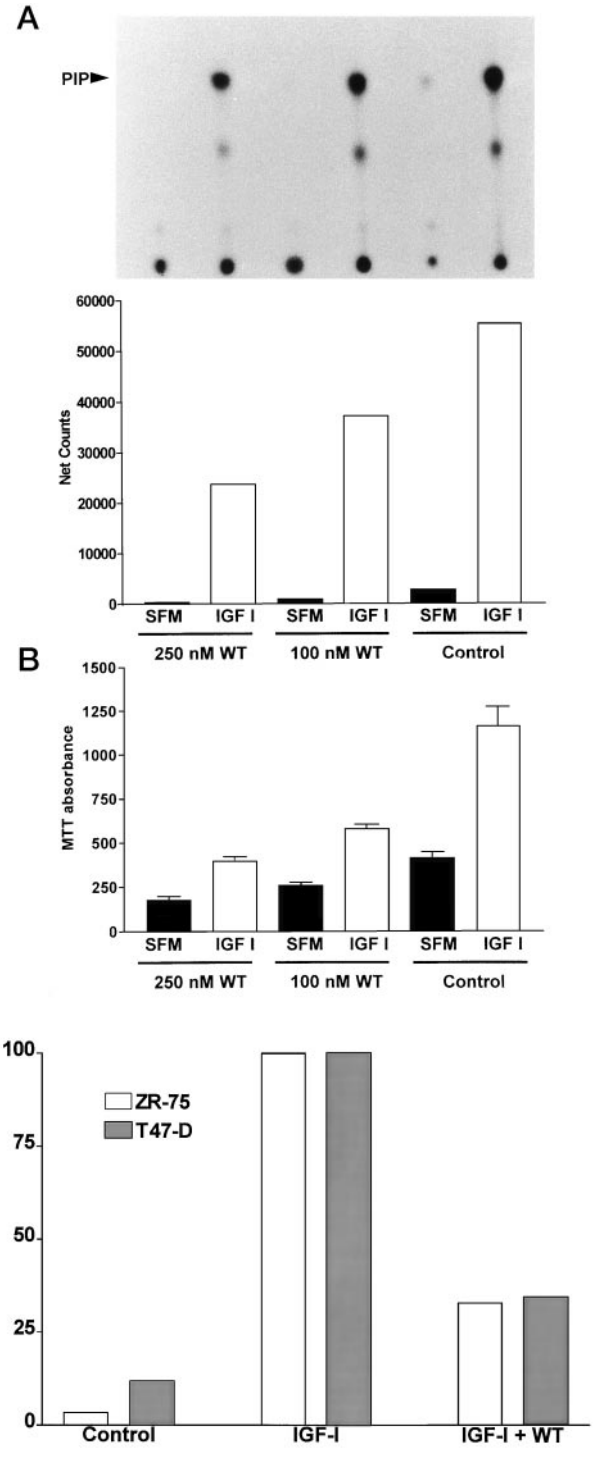

FIG. 7. **Wortmannin inhibits PI3 kinase activity and growth in MCF-7 cells.** MCF-7 monolayers were preincubated with wortmannin (*WT*) or Me_2SO alone (*Control*) as indicated. IGF-I was added (*open bars*) or not (*closed bars*) for 10 min, and cells were lysed, immunoprecipitated with IRS-1 antibody, and assayed for PI3 kinase activity as described under "Experimental Procedures." *A*, *top panel* shows autoradiogram of the TLC plate. Quantitation of individual spots (phosphatidylinositol phosphate (*PIP*)) is represented graphically. *B*, MCF-7 cells were plated at 40,000 cells/well, incubated in SFM overnight, and then preincubated for 30 min in the presence of wortmannin (*WT*) or Me_2SO alone (*Control*). IGF-I was added (*open bars*) or not (*closed bars*), and then MTT assay was performed after 3 days. *C*, wortmannin inhibits PI3 kinase activity in ZR-75 and T47-D cells. Cell monolayers were treated with 250 nM wortmannin and stimulated, and PI3 kinase assay was performed as in *A*. Individual spots representing phosphatidylinositol phosphate were quantitated and are expressed as a percentage of IGF-I stimulation.

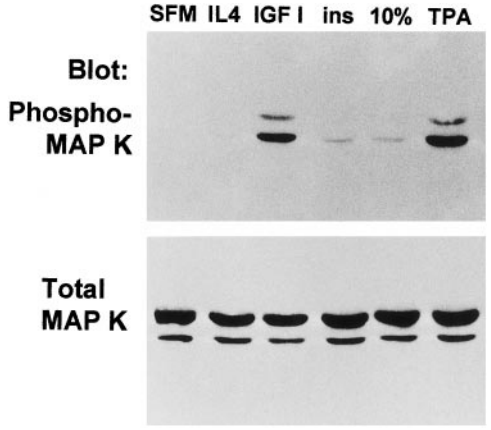

FIG. 8. **MAP kinase activation in MCF-7 cells.** MCF-7 monolayers were treated as indicated *above* lanes, and then TNESV lysates were separated by SDS-PAGE. Phospho-specific MAP kinase blotting (p44 and p42) was performed (*top panel*), followed by total MAP kinase blotting on the same membrane (*bottom panel*) to show equal loading.

we used 10-fold increased concentrations of each ligand and compared their effects on cellular signaling with IGF-I in MCF-7 cells. Excess IL-4 (IL-4, 10×) could not increase activation of IRS-1 (Fig. 10*A, top panel*), MAP kinase (Fig. 10*A, bottom panel*), or PI3 kinase (Fig. 10*B*) above the 50 ng/ml (IL-4, 1×) levels. In contrast, excess insulin enhanced activation of IRS-1 (Fig. 10*A, top*), MAP K (Fig. 10*A, bottom*) and PI3 kinase (Fig. 10*B*). Thus, excess insulin can activate MAP kinase and PI3 kinase to levels nearly equal to those achieved by IGF-I. We have found that 10 nM insulin does not activate the IGFR1 in MCF-7 cells (data not shown). However, excess insulin is known to activate both insulin receptor and IGFR1 (50). We suspect that the increase in activation of IRS-1 and MAP kinase by 100 nM insulin is mediated through activation of the IGFR1 and not by the insulin receptor.

DISCUSSION

Many of the IGF signaling pathways have been demonstrated in transfected cell lines or with *in vitro* assay systems. These studies have revealed that a complex network of signaling events are activated by IGFR1 and its adaptor proteins. Two homologous adaptor proteins, IRS-1 and IRS-2, were identified as substrates for the insulin receptor. In addition, these adaptor proteins are involved in signaling by other receptor types, including IGFR1 and the IL-4 receptor (14). In this study, we examined IRS-mediated signaling events in response to IGF-I, insulin, and IL-4 in three estrogen receptor-positive cell lines, MCF-7, ZR-75, and T47-D. In the IGF-I-unresponsive, estrogen receptor-negative cell lines MDA-231, MDA-468, MDA-435, and Hs-578T, very little or no IRS-1 activation was detected. Defects in the insulin/IGF signaling pathway have been previously documented in MDA-231 and MDA-468 cells (30, 31). Furthermore, Hs-578T cells do not express detectable IGFR1 mRNA (39). Thus, the physiologic role of IGF action in these ER− breast cancer cells is unclear.

Because IGF-I, insulin, and IL-4 are known to have divergent effects on ER+ breast cancer cells, functional signaling pathways must exist, and differences in activation of these pathways may account for the differences in biological activity. Because we found that both IRS-1 and IRS-2 were present in breast cancer cell lines and tumors, we hypothesized that the differential effects of the ligands could be due to differential activation of the adaptor proteins. Other studies have suggested that IRS-2 (originally named 4PS (IL-4-phosphorylated substrate) is the primary mediator of IL-4 effects in hematopoietic cells, and we reasoned that IRS-2 would have a similar

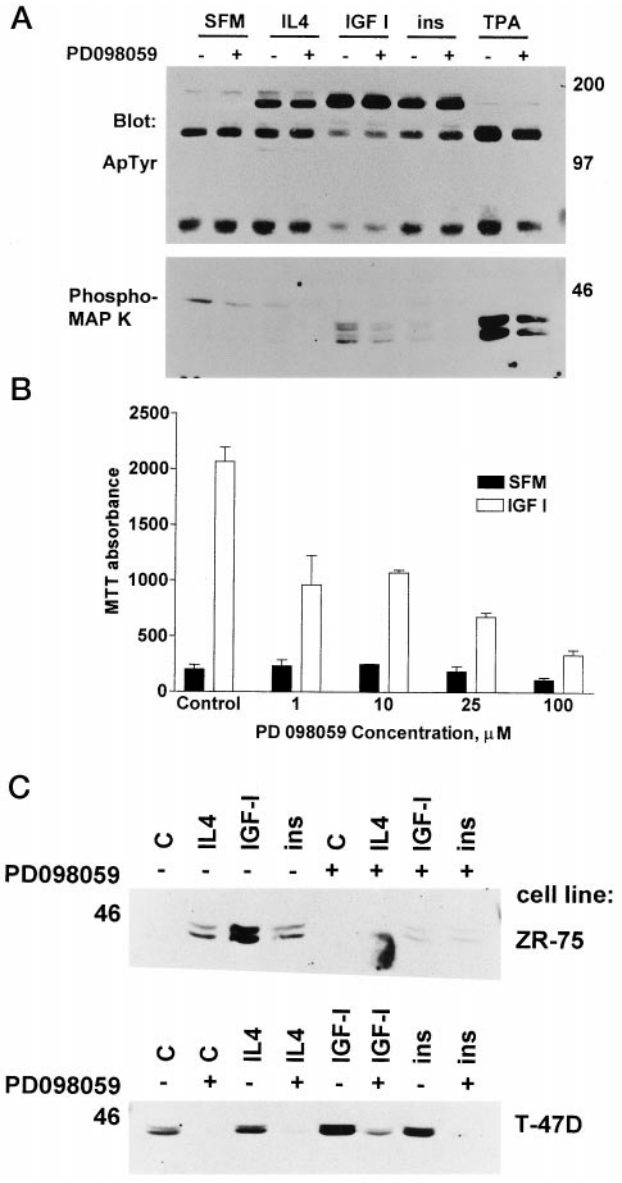

FIG. 9. **MAP kinase activating enzyme inhibitor PD098059 decreases IL-4-, IGF-I-, and insulin-stimulated MAP kinase activation and IGF-I stimulated growth in MCF-7 cells.** MCF-7 monolayers were preincubated for 30 min in the presence (+) or absence (−) of 25 μM PD098059, and then growth factor was added as indicated *above* lanes. *A*, TNESV lysates were separated by SDS-PAGE and blotted for anti-phosphotyrosine (*top panel*) and phospho-MAP kinase. Molecular weight markers are indicated at the *right* of each gel. *B*, MCF-7 cells were plated at 30,000 cells/well, serum starved overnight, and then preincubated for 30 min in the presence of PD098059 at the indicated concentration or Me_2SO alone (*Control*). IGF-I was added (*open bars*) or not (*closed bars*), and after 4 days, MTT assay was performed. *C*, MAP kinase activating enzyme inhibitor PD098059 decreases IL-4-, IGF-I-, and insulin-stimulated MAP kinase activation in ZR-75 and T47-D cells. ZR-75 (*upper panel*) and T47-D (*lower panel*) monolayers were preincubated in the presence (+) or absence (−) of 25 μM PD098059, and then lysates were immunoblotted for phospho-MAP kinase as in *A*, *lower panel*. Molecular weight markers are indicated at the *left* of each gel.

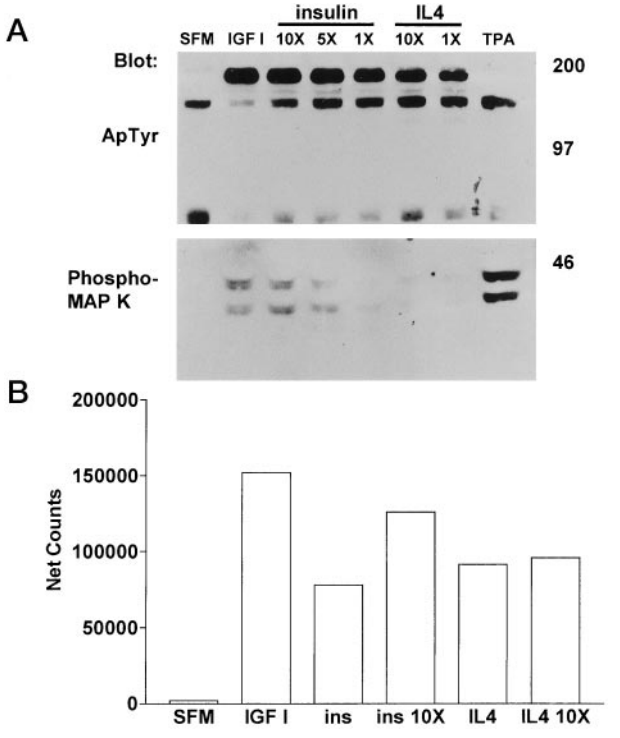

FIG. 10. **Excess IL-4 and insulin effects on IRS-1, MAP kinase, and PI3 kinase activation.** MCF-7 monolayers were treated with SFM alone, 5 nM IGF-I (*IGF I*), 100 nM insulin (*10×*), 50 nM insulin (*5×*), 10 nM insulin (*1×*), 500 ng/ml IL-4 (*10×*), 50 ng/ml IL-4 (*1×*), or 12-*O*-tetradecanoylphorbol-13-acetate (*TPA*) as indicated. *A*, TNESV lysates were separated by SDS-PAGE, and gels were blotted for anti-phosphotyrosine (*ApTyr, upper panel*) or phospho-MAP kinase (*lower panel*). *B*, lysates were immunoprecipitated with IRS-1 antibody and assayed for PI3 kinase activity as described under "Experimental Procedures." Quantitation of individual phosphatidylinositol phosphate spots is represented in the graph. *ins*, insulin.

function in breast cancer cells. To our surprise, we discovered that IRS-2 is not the predominant substrate for IGF-I, insulin, or IL-4 receptors in MCF-7 or ZR-75 cells or for the IGF-I receptor in T47-D cells. Instead, IRS-1 appears to be the predominant signaling molecule activated by all three ligands. Furthermore, we found that IGF-I stimulated increased phosphotyrosine on IRS-1 compared with IL-4 or insulin, as evidenced by the slower migration of IGF-I-stimulated IRS-1 in all three cell lines and phosphotyrosine blotting of V-8-digested IRS-1 in MCF-7 cells.

IRS-1 has over 20 potential tyrosine phosphorylation sites, which serve as binding sites for SH2 domain-containing proteins. These phosphorylated sites provide docking positions for a wide array of other signaling molecules, such as PI3 kinase, Grb 2, and Syp, creating the possibility of a complex, multidimensional signal sent to cells. In addition, IRS-1 can also activate signaling pathways in the absence of tyrosine phosphorylation (40). Although there have been many reports of differential IRS signaling in different cell types, there have been few reports on differential signaling through IRS-1 in the same cell by different ligands (35). Our data support the possibility that the level of IRS-1 tyrosine phosphorylation and coupling to downstream signaling pathways is dependent on the receptor type.

Like other cells, activation of IRS-1 in breast cancer cells results in the downstream activation of several different signaling pathways. Although PI3 kinase has been shown to mediate the metabolic effects of insulin (41), our studies suggest that PI3 kinase also mediates IGF-I mitogenic effects in breast cancer cells. In addition, MAP kinase also apparently regulates IGF-mediated mitogenesis. Dufourny *et al.* (42) recently showed a 40% reduction in IGF-I-stimulated growth in MCF-7 cells using 20 μM PD098059. Despite this reduction, the authors concluded that MAP kinase was not required for mitogenesis because cyclin D1 expression and the hyperphosphorylation of Rb was not affected (42). Our inhibition of growth was similar (50–60%), but we did not study effects on gene expres-

sion distal to MAP kinase. Dufourny *et al.* (42) also used detection of up-shifted ERK2 as a marker for MAP kinase activation, whereas we used phosphospecific MAP kinase antibody. Our reduction in growth was greater than theirs, and we were also unable to completely inhibit activation of MAP kinase, suggesting that phospho-specific MAP kinase antibody may be more sensitive in detecting activated MAP kinase. However, in both studies, when PD098059 was given with IGF-I, growth was inhibited. Thus, it is possible that MAP kinase contributes to the mitogenic pathway and utilizes downstream molecules other than Rb and cyclin D1 to affect proliferation.

The central role of IRS-1 in breast cancer growth regulation has also been shown in transfection studies of MCF-7 cells. IRS-1 introduced into these cells results in enhanced cell growth and partial estrogen independence (43). Furthermore, we have shown that high IRS-1 levels were associated with early recurrence in node-negative breast cancer (21). Thus, IRS-1 is a key signaling molecule in breast cancer cells and initiates several mitogenic pathways. To interfere with IGF-mediated mitogenesis in breast cancer cells, targeting of IRS-1, or at steps proximal to its activation, could be an effective inhibitor of growth. Recently, studies using IRS-1 deficient fibroblasts have shown that expression of IRS-1 is not necessary for activation of MAP kinase (44). Unlike our cells, these fibroblasts phosphorylate IRS-2 and Shc after IGF-I exposure, suggesting that cells of different origins may utilize different downstream signaling pathways to mediate IGF effects.

Studies have shown that IL-4 is an inhibitor of breast cancer cell proliferation (19, 20). Moreover, IL-4 inhibits estradiol-mediated growth of estrogen-responsive cells. This is in distinct contrast to the effects of IGF-I on breast cancer cell growth. IGF-I alone is a mitogen, and IGF-I plus estradiol results in additive, if not synergistic, growth effects (45). Because we did not detect any qualitative differences between IGF-I and IL-4 signaling via IRS-1 and IRS-2, several possible explanations for these differences may exist. First, it has been suggested that different subcellular localization of IRS-1 and PI3 kinase is responsible for different signals delivered by insulin and platelet-derived growth factor in 3T3 L1 adipocytes (46). However, after fractionation of subcellular compartments (47), we were unable to detect any differences in the subcellular localization of IRS-1, PI3 kinase, and MAP kinase in MCF-7 or ZR-75 cells after stimulation with IGF-I, IL-4 and insulin (data not shown). Second, initiation of mitogenesis may require the crossing of an activation threshold of downstream signaling molecules. Thus, IGF-I is a mitogen because of its ability to more vigorously activate MAP kinase and PI3 kinase. If activation of the these pathways is less than optimal, as is the case for IL-4 and insulin stimulation or after wortmannin and PD098059 treatment, then the mitogenic response is similarly dampened. Although this may explain why IL-4 is not a mitogen, it does not readily explain how IL-4 could function to inhibit estradiol growth stimulation. Third, other pathways may also be activated by IL-4. It is well known that the JAK/stat pathway is required for IL-4 function in lymphocytes, and activation of these pathways could potentially be inhibitory in breast cancer cells (48). We have found that IRS-1 co-immunoprecipitates with JAK3 antibody in MCF-7 cells (data not shown). IL-4 could also activate other members of the MAP kinase family, such as stress-activated protein kinase/jun kinase or p38. Both of these signaling pathways have been implicated in programmed cell death (49), and activation of these pathways could account for the inhibitory effects of IL-4 on breast cancer cells.

Thus, IRS-1, and not IRS-2, is a key signaling molecule for IGFR1 in estrogen receptor-positive breast cancer cells. IGFR1 is a more potent activator of IRS-1 than either insulin or IL-4 receptor. We also observed a direct correlation between levels of IRS-1 tyrosine phosphorylation, activation of PI3 kinase and MAP kinase, and cell growth. We suspect that IGFR1 creates additional or different SH2 binding sites on IRS-1 that enhance activation of downstream signaling molecules. Neither insulin or IL-4 could effectively activate these downstream signaling pathways through IRS-1, and they are, therefore, less efficient promoters of cell growth. We conclude that signaling through IRS-1 is responsible for the mitogenic effects of IGF-I in estrogen receptor-positive breast cancer cell lines.

Acknowledgments—We thank Goutam Ghosh-Choudhury and Adrian V. Lee for helpful discussion and advice.

REFERENCES

1. Lee, A. V., and Yee, D. (1995) *Biomed. Pharmacother.* **49,** 415–421
2. Bates, P., Fisher, R., Ward, A., Richardson, L., Hill, D. J., and Graham, C. F. (1995) *Br. J. Cancer* **72,** 1189–1193
3. Cullen, K. J., Yee, D., Sly, W. S., Perdue, J., Hampton, B., Lippman, M. E., and Rosen, N. (1990) *Cancer Res.* **50,** 48–53
4. Blakesley, V. A., Kalebic, T., Helman, L. J., Stannard, B., Faria, T. N., Roberts, C. T., and Leroith, D. (1996) *Endocrinology* **137,** 410–417
5. O'Connor, R., Kauffmann-Zeh, A., Liu, Y. M., Lehar, S., Evan, G. I., Baserga, R., and Blattler, W. A. (1997) *Mol. Cell. Biol.* **17,** 427–435
6. Li, S., Resnicoff, M., and Baserga, R. (1996) *J. Biol. Chem.* **271,** 12254–12260
7. Osborne, C. K., Bolan, G., Monaco, M. E., and Lippman, M. E. (1976) *Proc. Natl. Acad. Sci. U. S. A.* **73,** 4536–4540
8. Lammers, R., Gray, A., Schlessinger, J., and Ullrich, A. (1989) *EMBO J.* **8,** 1369–1375
9. Sun, X. J., Rotenberg, P., Kahn, C. R., Backer, J. M., Araki, E., Wilden, P., Cahill, D. A., Goldstein, B. J., and White, M. F. (1991) *Nature* **352,** 73–77
10. Dey, B. R., Frick, K., Lopaczynski, W., Nissley, S. P., and Furlanetto, R. W. (1996) *Mol. Endocrinol.* **10,** 631–641
11. Sun, X. J., Wang, L.-M., Zhang, Y., Yenush, L., Myers, M. G., Jr., Glasheen, E., Lane, W. S., Pierce, J. H., and White, M. F. (1995) *Nature* **377,** 173–177
12. Beitner-Johnson, D., and LeRoith, D. (1995) *J. Biol. Chem.* **270,** 5187–5190
13. O'Neill, T. J., Rose, D. W., Pillay, T. S., Hotta, K., Olefsky, J. M., and Gustafson, T. A. (1996) *J. Biol. Chem.* **271,** 22506–22513
14. Yenush, L., and White, M. F. (1997) *Bioessays* **19,** 491–500
15. Lavan, B. E., Fantin, V. R., Chang, E. T., Lane, W. S., Keller, S. R., and Lienhard, G. E. (1997) *J. Biol. Chem.* **272,** 21403–21407
16. Lavan, B. E., Lane, W. S., and Lienhard, G. E. (1997) *J. Biol. Chem.* **272,** 11439–11443
17. Keegan, A. D., Nelms, K., White, M., Wang, L. M., Pierce, J. H., and Paul, W. E. (1994) *Cell* **76,** 811–820
18. Sun, X. J., Pons, S., Wang, L. M., Zhang, Y. T., Yenush, L., Burks, D., Myers, M. G., Glasheen, E., Copeland, N. G., Jenkins, N. A., Pierce, J. H., and White, M. F. (1997) *Mol. Endocrinol.* **11,** 251–262
19. Toi, M., Bicknell, R., and Harris, A. L. (1992) *Cancer Res.* **55,** 275–279
20. Blais, Y., Gingras, S., Haagensen, D. E., Labrie, F., and Simard, J. (1996) *Mol. Cell. Endocrinol.* **121,** 11–18
21. Rocha, R. L., Hilsenbeck, S. G., Jackson, J. G., Van Den Berg, C. L., Weng, C.-N., Lee, A. V., and Yee, D. (1997) *Clin. Cancer Res.* **3,** 103–109
22. Laemmli, U. K. (1970) *Nature* **227,** 680–685
23. Cleveland, D. W. (1983) *Methods Enzymol.* **96,** 222–229
24. Choudhury, G. G., Biswas, P., Grandaliano, G., Fouqueray, B., Harvey, S. A., and Abboud, H. E. (1994) *Kidney Int.* **46,** 37–47
25. Twentyman, P. R., and Luscombe, M. (1987) *Br. J. Cancer* **56,** 279–285
26. Engel, L. W., Young, N. A., Tralka, T. S., Lippman, M. E., O'Brien, S. J., and Joyce, M. J. (1978) *Cancer Res.* **38,** 3352–3364
27. Keydar, I., Chen, L., Karby, S., Weiss, F. R., Delarea, J., Radu, M., Chaitcik, S., and Brenner, H. G. (1979) *Eur. J. Cancer* **15,** 659–670
28. Yee, D., Cullen, K. J., Paik, S., Perdue, J. F., Hampton, B., Schwartz, A., Lippman, M. E., and Rosen, N. (1988) *Cancer Res.* **48,** 6691–6696
29. Myal, Y., Shiu, R. P. C., Bhaumick, B., and Bala, M. (1984) *Cancer Res.* **44,** 5486–5490
30. Costantino, A., Milazzo, G., Giorgino, F., Russo, P., Goldfine, I. D., Vigneri, R., and Belfiore, A. (1993) *Mol. Endocrinol.* **7,** 1667–1676
31. Sepp-Lorenzino, L., Rosen, N., and Lebwohl, D. E. (1994) *Cell Growth Differ.* **5,** 1077–1083
32. Tartare-Deckert, S., Sawka-Verhelle, D., Murdaca, J., and Van Obberghen, E. (1995) *J. Biol. Chem.* **270,** 23456–23460
33. Pruett, W., Yuan, Y., Rose, E., Batzer, A. G., Harada, N., and Skolnik, E. Y. (1995) *Mol. Cell. Biol.* **15,** 1778–1785
34. Harada, S., Smith, R. M., Smith, J. A., White, M. F., and Jarett, L. (1996) *J. Biol. Chem.* **271,** 30222–30226
35. Wang, L.-M., Myers, M. G., Jr., Sun, X.-J., Aaronson, S. A., White, M. F., and Pierce, J. H. (1993) *Science* **261,** 1591–1594
36. Yano, H., Nakanishi, S., Kimura, K., Hanai, N., Saitoh, Y., Fukui, Y., Nonomura, Y., and Matsuda, Y. (1993) *J. Biol. Chem.* **268,** 25846–25856
37. Myers, M. G., Jr., Wang, L.-M., Sun, X.-J., Zhang, Y., Yenush, L., Schlessinger, J., Pierce, J. H., and White, M. F. (1994) *Mol. Cell. Biol.* **14,** 3577–3587
38. Pang, L., Sawada, T., Decker, S. J., and Saltiel, A. R. (1995) *J. Biol. Chem.* **270,** 13585–13588
39. Yee, D., Lebovic, G. S., Marcus, R. R., and Rosen, N. (1989) *J. Biol. Chem.* **264,** 21439–21441

40. Myers, M. G., Zhang, Y. T., Aldaz, G. A. I., Grammer, T., Glasheen, E. M., Yenush, L., Wang, L. M., Sun, X. J., Blenis, J., Pierce, J. H., and White, M. F. (1996) *Mol. Cell. Biol.* **16,** 4147–4155
41. Okada, T., Kawano, Y., Sakakibara, T., Hazeki, O., and Ui, M. (1994) *J. Biol. Chem.* **269,** 3568–3573
42. Dufourny, B., Alblas, J., van Teeffelen, H. A. A. M., van Schaik, F. M. A., van der Burg, B., Steenbergh, P. H., and Sussenbach, J. S. (1997) *J. Biol. Chem.* **272,** 31163–31171
43. Surmacz, E., and Burgaud, J.-L. (1995) *Clin. Cancer Res.* **1,** 1429–1436
44. Bruning, J. C., Winnay, J., Cheatham, B., and Kahn, C. R. (1997) *Mol. Cell. Biol.* **17,** 1513–1521
45. McGuire, W. L., Jr., Jackson, J. G., Figueroa, J. A., Shimasaki, S., Powell, D. R., and Yee, D. (1992) *J. Natl. Cancer Inst.* **84,** 1336–1341
46. Ricort, J.-M., Tanti, J.-F., Van Obberghen, E., and Le Marchand-Brustel, Y. (1996) *Eur. J. Biochem.* **239,** 17–22
47. Coligan, J. E., Dunn, B. M., Ploegh, H. L., Speicher, D. W., and Wingfield, P. T. (1997) *Current Protocols in Protein Science*, John Wiley & Sons, New York
48. Kotanides, H., Moczygemba, M., White, M. F., and Reich, N. C. (1995) *J. Biol. Chem.* **270,** 19481–19486
49. Johnson, N. L., Gardner, A. M., Diener, K. M., Lange-Carter, C. A., Gleavy, J., Jarpe, M. B., Minden, A., Karin, M., Zon, L. I., and Johnson, G. L. (1996) *J. Biol. Chem.* **271,** 3229–3237
50. Flier, J. S., Usher, P., and Moses, A. C. (1986) *Proc. Natl. Acad. Sci. U. S. A.* **83,** 664–668